

**INVESTIGATIONS ON ACOUSTIC EMISSIONS
IN SOFTWOOD CRACK INITIATION AND GROWTH**

**UNTERSUCHUNGEN ÜBER SCHALLEMISSIONEN BEIM
ANRISS UND RISSFORTSCHRITT IN NADELHOLZ**

**RECHERCHES SUR DES EMISSIONS ACOUSTIQUES
A L'INITIATION ET PROPAGATION DES FISSURES
EN BOIS RESINEAUX**

Simon Aicher

Christian Große

Murat Gappoev

SUMMARY

Introductory a brief review of nondestructive testing applied to wood based on acoustic waves with special consideration to acoustic emission (AE) measurements is given. The paper then describes first evaluations of tests monitoring AEs from crack initiation and propagation along grain of spruce due to tension perpendicular to grain. The tests in RL-crack system were conducted with a fracture mechanics SENB specimen. The AE events were captured as complete signals by piezo-electric transducers, pre-amplification and a transient recorder.

The tests revealed AE events with relatively extra large peak amplitudes followed by stiffness nonlinearities below maximum load. Repeatedly occurring signals of comparable shape, possibly bound to specific fracture phenomena, were registered. Further experiments with thorough waveform parameter evaluation especially at proof testing stress levels might lead to better tools for nondestructive strength assessment of structural timber components.

ZUSAMMENFASSUNG

Es wird ein Abriß über die zerstörungsfreie Prüfung von Holz mittels akustischer Wellen, insbesondere im Hinblick auf Schallemissions(AE-)messungen gegeben. Im Anschluß daran wird über erste Auswertungen von Versuchen zur Aufzeichnung von Schallemissionen bei Rißinitiiierung und -fortschritt in Fichtenholz parallel zur Faserrichtung infolge Querkzugbeanspruchung berichtet. Die Versuche wurden im RL-Rißsystem mit einem Bruchmechanik-SENB-Prüfkörper durchgeführt. Die Erfassung der Schall-

emissionsereignisse, als komplette Signale, erfolgte mittels piezo-elektrischer Aufnehmer, Vorverstärkung und Transientenrecorder.

Die höchsten Schallereignis-Spitzenamplituden mit anschließenden Steifigkeits-Nichtlinearitäten wurden unterhalb der Maximallast gemessen. Es wurden wiederholt Signale vergleichbarer Form aufgezeichnet, die vermutlich an spezifische Bruchvorgänge geknüpft sind. Weitere Untersuchungen mit eingehender Auswertung der Wellenformparameter, insbesondere im Bereich von »Proof-test«-Spannungsniveaus, dienen der Zielsetzung einer verbesserten zerstörungsfreien Prüfung tragender Holzbauteile.

RESUME

Un abrégé est donné sur des essais non-destructifs par ondes acoustiques réalisés sur du bois, tenant compte spécialement de mesures par émissions acoustiques. Un rapport est donné sur les interprétations des investigations aux émissions acoustiques à l'occasion de l'initiation et de la propagation des fissures parallèles à l'orientation des fibres dans le bois de sapin par suite d'efforts de traction perpendiculaires à la fibre. Les essais ont été réalisés dans le système de fracture RL avec une éprouvette SENB de mécanique de rupture. Les événements acoustiques en tant que signaux complets ont été enregistrés par des récepteurs piézo-électriques, préamplification et recorder aux signaux transients.

Les amplitudes à pointe d'événements acoustiques, suivies de non-linéarités de rigidité, ont été mesurées en-dessous de la charge maximum. A maintes reprises des signaux de formes comparables, probablement en corrélation avec des événements de ruptures spécifiques, ont été enregistrés. D'autres investigations seront réalisées évaluant les paramètres de forme d'onde, en particulier au niveau de contraintes de »Proof-test« et avec le but d'une inspection non-destructive améliorée des éléments portants de bois.

Key-words: Nondestructive testing of wood, acoustic emission measurement, fracture mechanics SENB specimen, waveform parameter evaluation

1. Introduction

The paper reports on general aspects, aims and some first results in nondestructive testing of timber, especially by means of acoustic emission measurement. The investigations are part of an extensive research project on timber fracture mechanics aiming at a deepened knowledge of timber fracture in general as well as more reliable timber structures. The research is conducted by Otto-Graf-Institute in cooperation with Institute of Building Materials of University of Stuttgart and represents one of the more recently established branches of the interdisciplinary research project SFB 230 »natural constructions« funded by the Deutsche Forschungsgemeinschaft and located at Universities of Stuttgart and Tübingen.

2. NDE methods based on acoustic waves

Three major nondestructive evaluation (NDE) methods based on recording of elastic (acoustic or stress) waves in the ultrasonic range propagating through materials can be differentiated. The most frequently used method is based on measurement of transit time of the fastest component of a compression wave induced into the material by a more or less undefined impact. The basic principle of evaluation consists in the dependency of transit time, i. e. wave (sound) speed and material constitutive law resp. density. Via comparison to perfect states, travel times can be correlated to imperfect material states. The method is rather simple, but nevertheless provides in many applications, especially assessment of wood decay by fungi sufficiently accurate results (i. a. Anthony and Bodig, 1989; Pellerin, 1989).

Another related but more sophisticated NDE method is ultrasonic pulse measurement. Instead of a random impact, a defined signal is induced into the material by means of an ultrasonic pulser. The evaluation may consist purely in measurement of transit time but can also comprise changes of waveform parameters such as maximum amplitude, frequency, centroid time. The method allows detection of timely rather stable imperfect states, i. a. of fungus decay (Patton-Mallory and De Groot, 1989) but also monitoring and interpretation of fast changing situations, such as crack growth (Reinhardt and Hordijk, 1988). The third method, focused on in this paper deals with measurement of acoustic emissions (AEs) emitted from stressed materials during initiation and propagation of (micro-)cracks which cause distinct energy releases and so forth elastic (acoustic) waves.

3. AE in wood science

A scientific proof of elastic waves emitted from highly stressed wood was given by the fundamental work of Kaiser (1950). In the Sixties Porter (1964), Debaise et al. (1966) and Adams (1969) conducted first studies mainly on softwoods stressed parallel to grain with then advanced tools as piezo-electric transducers, amplifiers, high pass filters and electronic counters. It was observed that tension, bending and cleavage results in AEs at quite low strain levels, whereas compression loading produces only few emissions. In bending at proportional limit a marked increase in count rate, indicating progressive damage, was detected.

Porter et al. (1972) worked on AE based assessment of finger joint failure. The AE method was found well apt for anticipating failure loads. Use of count rates (pulse increment per load increment) at approx. 50 % strength level gave failure estimations with 10 % error. The error percentage steadily decreased with count rates from increasing stress levels, resulting in a 5 % error at 80 % strength level.

Ansell (1982) performed tension parallel to grain tests with different softwoods confirming prior results, i. e. low pulse rates at small strains and high emission rates close to failure. Further, AE-strain curves were directly related to the annual ring structure. Pulse sum was not found to be significantly correlated with strength.

Until mid-Eighties AE testing in wood science meant pulse counting, i. e. registration of crosses of predefined voltage thresholds. Beall (1986) then introduced the evaluation of bursts events and peak amplitudes in investigations on internal bond behaviour of particleboard. Similar to pulse sum results from solid wood no significant correlation between total events to failure and strength was found, however, an excellent correlation between number of nominal half-total events and strength. Beall also showed that at least the investigated particle board, alike many composites, did not obey the so-called Kaiser effect in reversed loading cycles but showed a rather constant Felicity ratio of about 0.9 until failure.

Noguchi et al. (1991) successfully employed AE monitoring to location of even incipient stages of termite attack on wood resp. commercial dimension lumber. Rate of events and waveform parameters such as event peak amplitudes and rise time were evaluated.

In Germany later AE measurements applied to wood fracture are scarce. Recently, Niemz and Lühmann (1992) published results of pulse countings with different wood species; pulse sums were found uncorrelated.

4. Specimen and test set-up

The first orienting tests to monitor AEs emitted in wood fracture processes with crack propagation parallel to grain were conducted with single edge notched (SENB) specimens made from spruce loaded in three point bending. Specimen shape and test set-up followed a draft standard concerning determination of fracture energy of wood in tension perpendicular to the grain direction (Gustafsson and Larsen, 1989). Fig. 1 shows the specimen, respective dimensions and load application configuration. The specimen consists of three parts glued together: the mid-located actually tested notched fracture mechanics volume with grain direction normal to bending tensile stresses and two side-studs with horizontal grain direction. The crack system investigated is termed RL-system where R ($\hat{=}$ radial growth direction) denotes the axis normal to the crack plane and L ($\hat{=}$ longitudinal growth direction) specifies the crack propagation direction. The fracture volume which had been conditioned until weight equilibrium in a climate of 20 °C and 65 % relative humidity, was middle European spruce with a density of 420 kg/m³ at 12 % moisture content and the average growth ring width was 1.8 mm.

Fig. 2 shows the test set-up. The deformation controlled bending tests were performed in a screw driven 20 kN testing machine (ZWICK 1454). The cross-head speed counted 0.4 mm/min in order to achieve peak load nominally three minutes after begin of loading. For acquisition of accurate load data, in view of the very small maximum loads (160 – 220 N), an extra 1 kN load cell was used, fixed between cross-head and loading point. Besides load and AE data, load point deflection and crack opening displacement were registered continuously by a computerized data logger.

5. AE data capture equipment

Two equal piezo-electric broadband transducers were employed. The coupling of the transducers to the specimen, at this stage, was performed with ordinary pastillin and fixation, to prevent fall off, was realized with a rubber band (Fig. 3). The used couplant is possibly not the best apt what will be elaborated in further investigations. The points

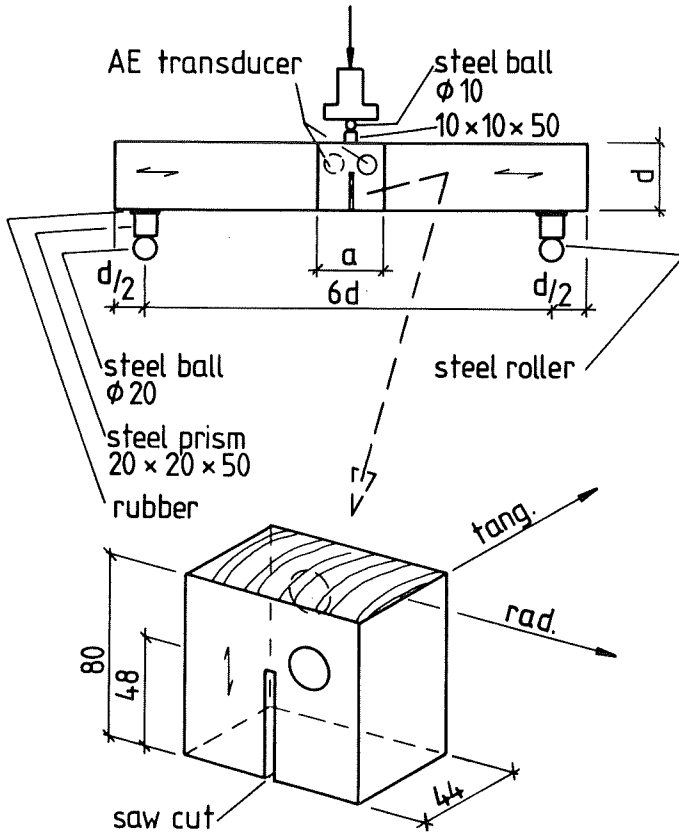


Fig. 1 Investigated single edge notched bending (SENB) specimen and test arrangement

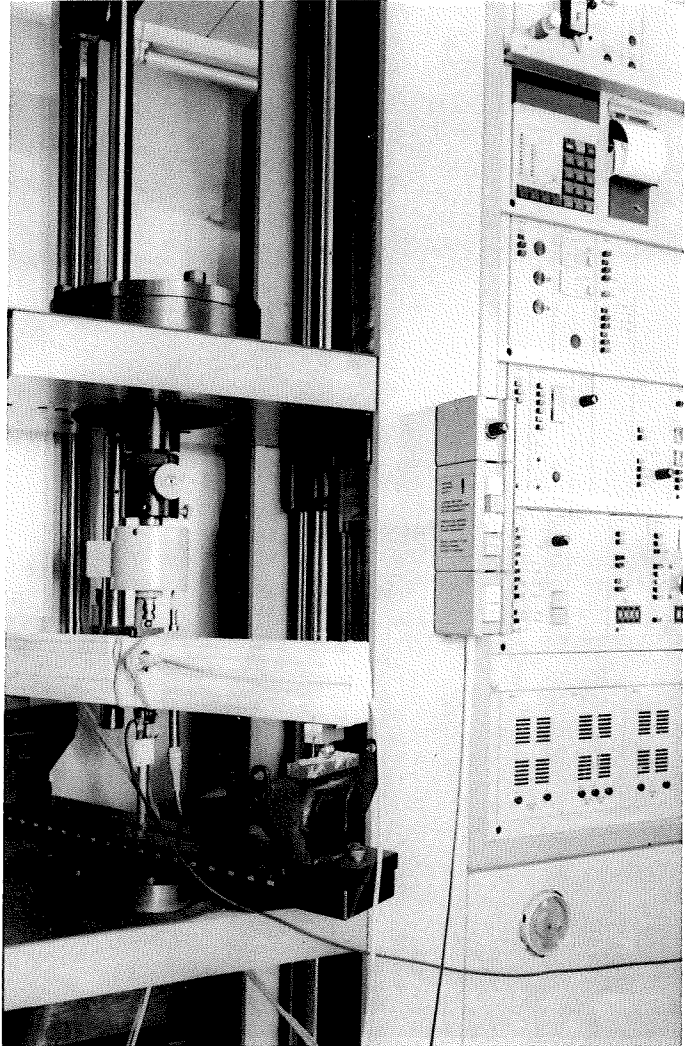


Fig. 2 Test set-up

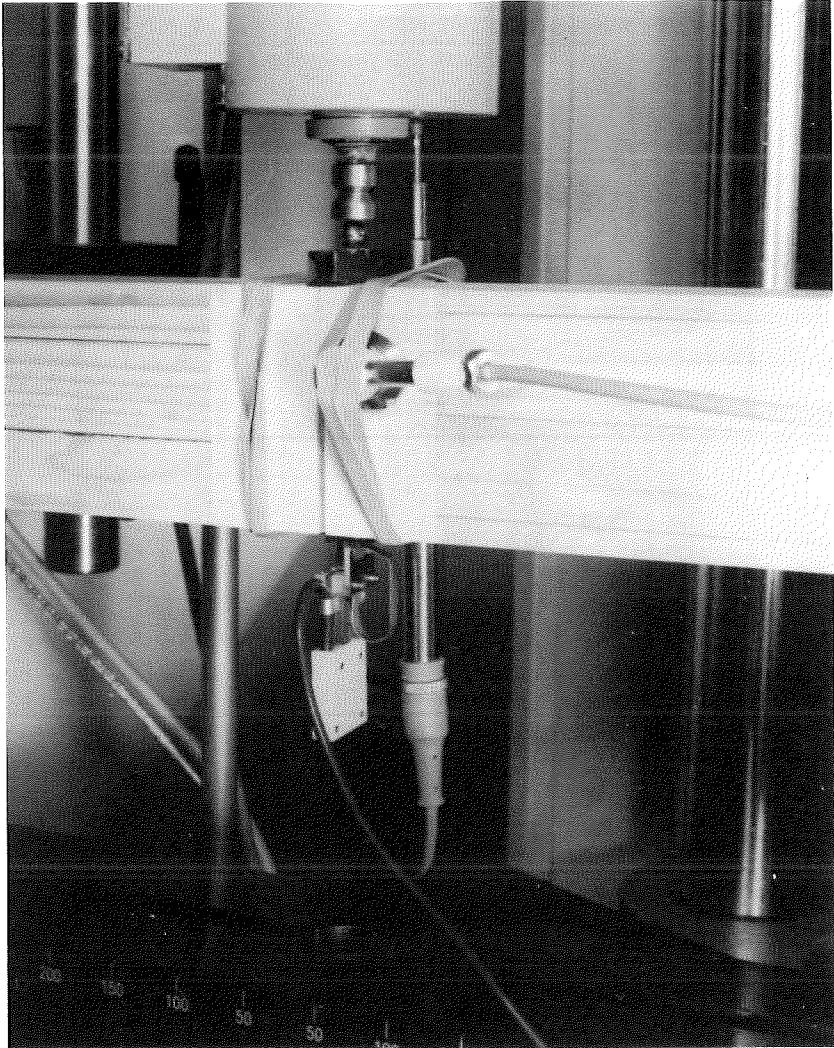


Fig. 3 Detail of test set-up with AE-transducers and crack opening COD gauge

of application of the two transducers were located on diagonally opposite sides of the specimen close to the developing crack plane (Figs. 1 and 3).

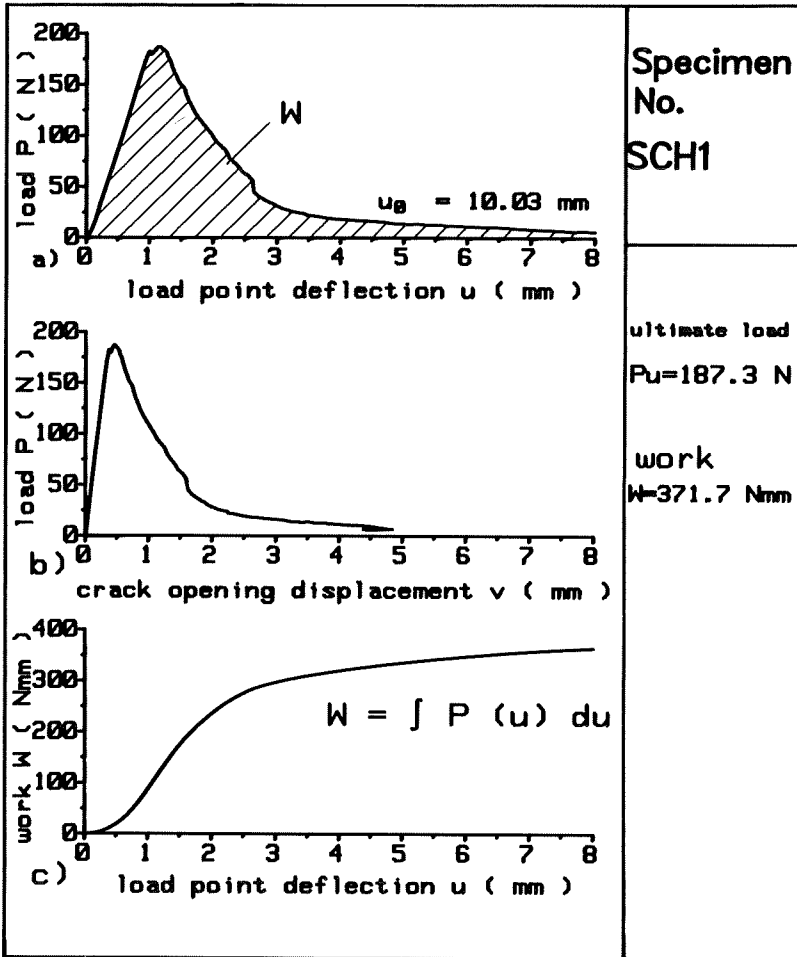
Due to the highly attenuating material amplification of the signals by means of a pre-amplifier was necessary. The recording of the AEs was not performed with a standard AE recording system, usually only able to extract a set of parameters of a signal, such as trigger time, signal duration, rise time, max. amplitude etc., but by a fast transient recorder. The latter equipment captures the complete signal. The employed computer-controlled recorder had a 1 MHz A/D converter and an internal memory for each of eight channels. For a more detailed description of the equipment, see Große (1991).

A then limiting factor for the tests reported were signal storage facilities which were restricted to 276 signals per experiment and channel. Said signal capturing capability is defined by the chosen trigger time of one millisecond. Trigger time means that the registered analog signals are stored in a dynamic memory according to length of trigger span (here 1 msec) and can be captured partially or totally in case a pulse within the individual trigger time exceeds threshold (or trigger) level. If no sufficiently high signal occurs the memory is purged. Through adequate settings of pre- and post-trigger ranges (in relative units of trigger time) defined signal parts before and after first threshold crossing can be submitted to evaluation. Through adequate pre-trigger range, i. a. exact analysis of signal rise time can be performed. Pilot tests revealed that length of burst events is nearly throughout less than 1 msec. In the results presented, pre- and post-trigger were set to 25 resp. 75 % and threshold level (compare chap. 6.2.1), equalled to 0.36 volt.

6. Test results

6.1 Load deflection behaviour and fracture energy

Figs. 4a, b give the test results for load point deflection and crack opening displacement of specimen No. SCH1. The load versus load point deflection curve is characterized by an almost linear relationship until a first significant load drop about 5 % below peak load. The latter pop-in, however, did not limit the linear relationship ultimately, as could be reasoned from Fig. 4a, but was already preceeded by a pronounced nonlinearity (compare Figs. 5 and 6). Following the pop-in a degressiv nonlinear bad



Figs. 4a - c Load-deformation test results

- a) load - load point deflection curve
- b) load - crack opening displacement curve
- c) work of applied load versus load point deflection

recovery until maximum load occurred and then a stable descending branch until complete separation followed.

The work W performed by the applied load P until complete failure was 372 Nmm (Fig. 4c). Taking into account the additional work contributed by beam weight in between span $G_1 = 8.92$ N, as well fixture resp. acoustic transmitter weight $G_2 = 1.42$ N fracture energy G_f , the total energy necessary to create one unit of crack area, came up to 390 N/mm. Fracture energy was computed from expression

$$G_f = [W + (G_1 + 2 G_2) u_0] / A_n \quad (1)$$

where $u_0 = 10.03$ mm is the deflection at complete separation and $A_n = 48 \times 44$ mm² is the net area of the uncracked specimen. Equ. (1) represents the recommended equation for Mode I fracture energy determination of mortar and concrete (RILEM, 1985) but is slightly different from Gustafsson and Larson's proposal for wood. There, the term $2 G_2 u_0$, the energy contribution of fixture weight is considered negligible and beam weight is not reduced by span to total length ratio.

The received load deflection curve resp. fracture energy of 232 N/m corresponds well to values obtained from extensive investigations on size effects with similar spruce specimens (Aicher, Gappoev and Reinhardt, 1993), so to say, fracture behaviour of the specimen can be regarded quite representative for spruce.

6.2 AE results

6.2.1 AE events, peak amplitudes

Fig. 5 shows the load-load point deflection curve until a deflection of 4 mm (right handside ordinate and upper abscissa) and secondly peak amplitudes (PAs) of recorded AE events along real testing time (left handside ordinate and lower abscissa). More precisely, each given PA represents the maximum PA of all individual events registered per test second by one of the two transducers, here channel one.¹

¹ The values for PAs of preamplified signals are given in volt and correct relatively to each other. A conversion into true displacement or a comparison with absolute values cited in literature are doubtful because of the significant influence of the individually realized transducer coupling.

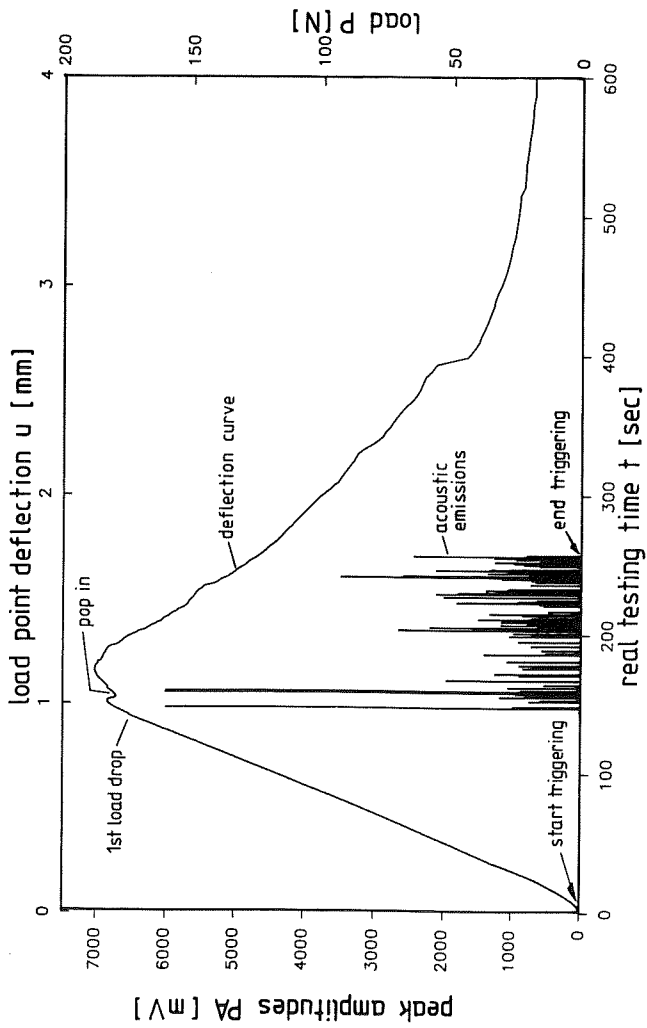


Fig. 5 Maximum peak amplitudes (PAs) of acoustic emission (AE) events versus test time and load deflection curve

The triggering, i. e. the recording of AE events was started at loading begin. In order not to register too many events before assessed peak load range, in view of the mentioned limited event storage facilities (276 events), threshold level was set to 0.36 volt. This value is rather high compared to literature where for ring down countings 0.1 volt is not uncommon.² In view of the latter it has to be pointed out that Fig. 5 might mislead to the idea that no burst events occurred before first peak amplitudes given. However, for sure is only that probable events were of less than 0.36 volt (after preamplification).

The end of the data capture is located well in the descending load deflection branch.

Fig. 6 gives an enlarged view of PAs in the time range between 140 to 260 sec. Each column in Fig. 6 represents the maximum PA of all events per time unit (1 sec), the number of events per individual time unit is given on top of the columns and the horizontal bars within the columns denote the PA values of all minor events. According to Fig. 6 the rate of events, i. e. number of events per unit time, varies between zero and eleven. PAs vary between roughly 0.5 volt and 6 volt. Fig. 6 visualizes that the three almost highest PAs, actually exceeding the dynamic range of the equipment, mark comparably significant stages in the load deflection curve. The first extra large PA and the two following ones coincide with changes in the load deflection behavior, i. e. stiffness changes, caused by progressive damage.

Further information on burst signal amplitudes is yielded in Fig. 7. The columns show the summed up PAs of all events per time unit and second, the curve of cumulative PAs of all burst events in the monitored range is given. The comparatively few events of mostly quite low PAs in the loading range from pop-in to about 95 % of peak load in the descending branch give rise to the assumption that the major fiber breakages happen well before peak load.

² In future tests specifically focussing on pre-peak signals specific consideration will be given to adequate thresholds also in view of always superimposed noise levels. Here noise ranged between ± 0.2 volt.

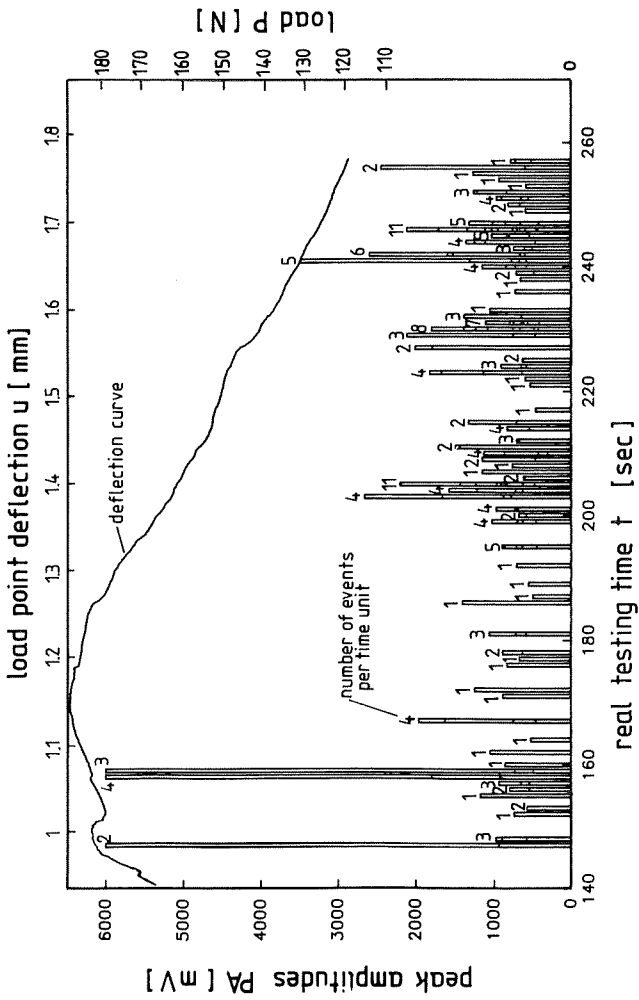


Fig. 6 Event peak amplitudes and AE event-time rates

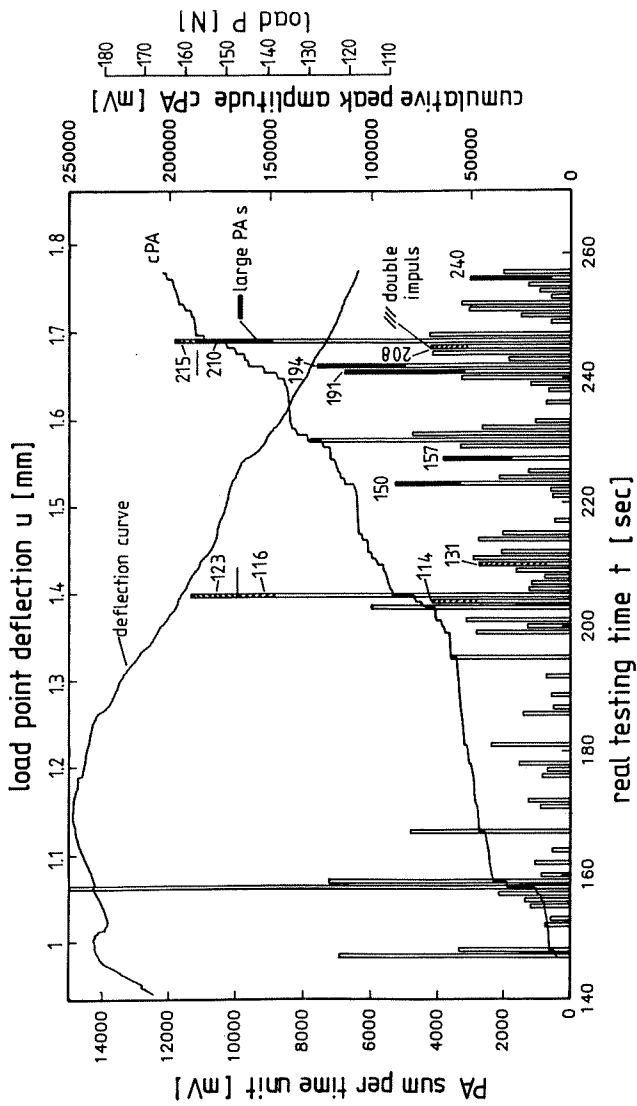


Fig. 7 Event PA sums per time unit (columns) and cumulative PA curve versus test time and load-deflection curve

6.2.2 Frequency analysis, waveform characteristics

So far the aspects of burst events looked at, were number and rates of events and with regard to the individual signal, only the event PA was considered. However, storage of the whole signal allows more insight. Further signal processing can be roughly separated in frequency analysis after signal transformation, waveform parameter evaluation and interpretation of shapes of waveforms.

Frequency analysis was performed by means of fast Fourier transformation (FFT). Fig. 8 gives an example of frequency evaluation of signal No. 80 occurred at test time 172 sec. Fig. 8a shows the received signal with amplitude distribution along time and Fig. 8b depicts the respective amplitude – frequency distribution. The frequencies in the ultra acoustic range stretch from 20 to roughly 300 kHz and the frequencies contributing most the energy of the signal are in the range of about 110 – 120 kHz. Due to the small number of signals yet evaluated, comparisons and conclusions would be overstating.

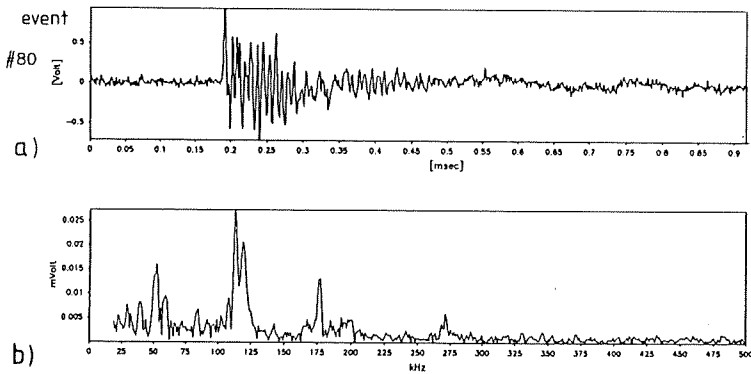


Fig. 8 Acoustic emission event No. 80
a) recorded waveform
b) computed amplitude-frequency distribution

Waveform parameters, suitable for signal description, besides PAs can be rise time, i. e. time from first threshold voltage crossing to PA or event duration, being time from first to last threshold crossing (compare Fig. 9). However, those parameters are still quite coarse as PAs depend profoundly on coupling and duration times depend on threshold (trigger) level. Ultimately, pure parameter extraction would not necessarily need signal storage.

The highest possible information can be received by considering the total shape of the burst signals, i. a. by means of image digitalization. Establishment of correlations between signal shapes and certain stages of stress strain relations or fracture are based on the assumption that certain failure mechanism in fibre separation emit distinct signal patterns.

The acoustic signals received, comprised expected rather amorphe signals but also some with indisputable similarities. In Fig. 7 two different types of post peaks AE events are denoted. The blackened column areas 150, 157, 191, 194, 210, 240 mark events of high PAs of 1.8 to 3.5 volt; the individual similar waveforms of the events are given in Fig. 9. Alike, the hatched signals in Fig. 7, so 114, 116, 123, 131, 208, 215, represent events, i. e. PAs of events, termed double impulses. As double impulse such an event was termed where time between PAs of two succeeding signals, which could be interpreted as separate events, occurred within the trigger time of 1 millisecond. The respective similar waveforms are given in Fig. 10. The time span between the two PAs varied roughly from 0.1 to 0.7 milliseconds.

7. Conclusions and research aims

First tests were conducted monitoring acoustic emissions (AEs) caused by crack initiation and propagation along grain due to tensile stresses perpendicular to grain (fracture mechanics RL crack system). The species was spruce, the specimen were single edge notched beams loaded in bending and the AEs were recorded by means of a fast transient recorder capturing the whole waveform. The tests revealed AE events with extra large peak amplitudes below maximum load which were followed by load displacement nonlinearities. Although waveform parameter and shape evaluation is not yet completed, the existance of acoustic events of comparable characteristics bound to probably specific micro-cracking phenomena can be stated. Generalization, however, is too early.

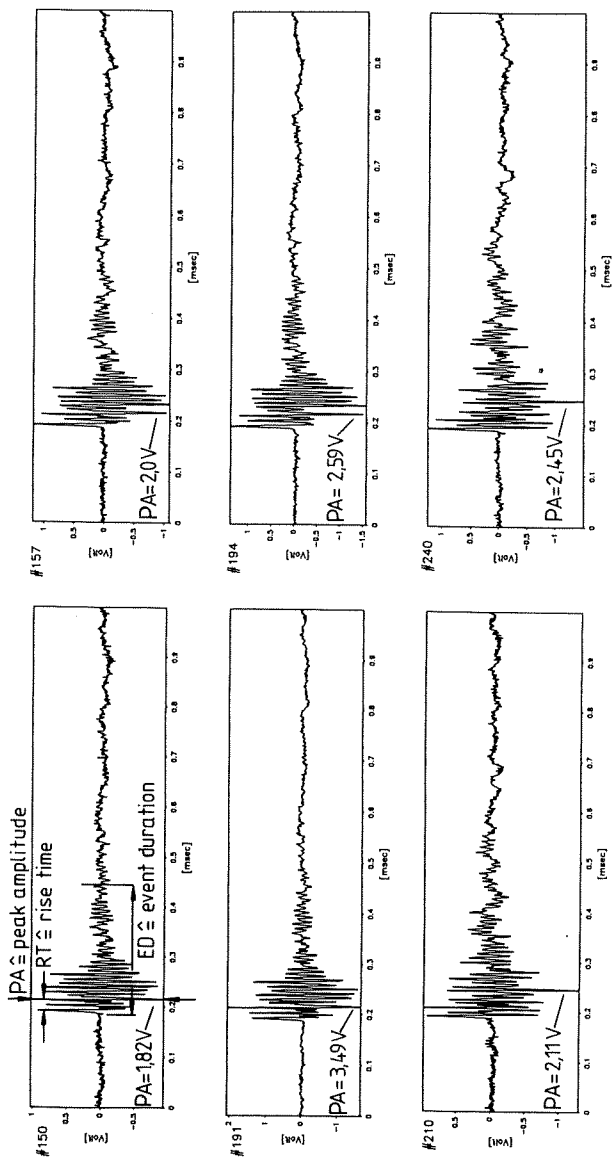


Fig. 9 Similar shaped waveforms of AE events with high peak amplitudes

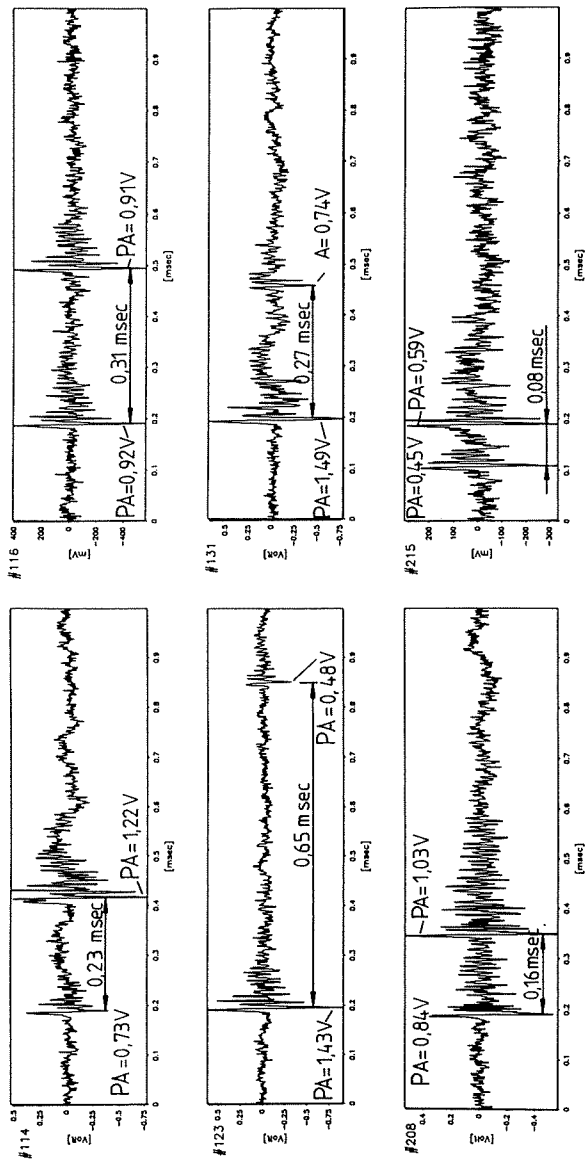


Fig. 10 Similar shaped waveforms of AE events termed double impulses

The aim of further research can be sketched as following: Generally a deepened insight in AEs from cracking processes in fracture mechanics relevant situations in wood is sought. The investigations focus on spruce, Mode I and RL, TL crack systems as well on glue lines of purely wooden and wood steel joints. Apart from pulse and event rate special attention will be paid to evaluation of waveform characteristics. Intention is to classify waveforms bound to initiation of (micro-)cracking. Acoustic emission tools shall be developed for nondestructive strength assessment, i. a. as a means of proof testing of structural timber components such as large finger joints and glued-in bolts.

8. Acknowledgements

It is gratefully acknowledged that the investigations are supported by the Deutsche Forschungsgemeinschaft DFG via funding project D7 »material oriented constructing with the natural material wood« as part of the Sonderforschungsbereich 230 »natural constructions« at Universities of Stuttgart and Tübingen.

Many thanks are indepted to the engaged help of technician Mrs. Silvia Brunold.

9. References

Adams, R. D. (1969): Fracture development in wood resulting from bending stresses and detected by using the acoustic emission phenomenon. Master Thesis, Dep. of Forestry, University of British Columbia

Aicher, S., Gappoev, M., Reinhardt, H. W. (1993): Maßstabgesetz und Bruchenergien von Fichte bei Zugbeanspruchung quer zur Faserrichtung. Holz als Roh- und Werkstoff (in press)

Ansell, M. P. (1982): Acoustic emission from softwoods in tension. Wood Science and Techn. 16: pp. 35 – 58

Anthony, R. W., Bodig, J. (1989): Nondestructive evaluation of timber structures for reliable performance. Proceedings Pacific Timber Eng. Conf., Vol. 2, pp. 197 – 200

Beall, F. C. (1986): Effect of resin content and density on acoustic emission from particleboard during internal bond testing. Forest Products Journal 36 (7/8), pp. 29 – 33

Debaise, G. R., Porter, A. W., Pentoney, R. E. (1966): Morphology and mechanics of wood fracture. *Mat. Res. Stds.*, pp. 493 – 499

Große, C. (1991): Detection of cracks in reinforced concrete – an introduction to the problem with some measurements. *Otto-Graf-Journal*, Vol. 2, pp. 72 – 90

Gustafsson, P. J., Larsen, H. J. (1989): Determination of the fracture energy of wood for tension perpendicular to the grain (draft standard). In: Design of endnotched beams, CIB paper W-18A/22-10-1, Berlin

Kaiser, J. (1950): Untersuchungen über das Auftreten von Geräuschen beim Zugversuch. Ph. D. Thesis, Technical University Munich

Niemz, P., Lühmann, A. (1992): Anwendung der Schallemissionsanalyse zur Beurteilung des Bruchverhaltens von Holz und Holzwerkstoffen. *Holz als Roh- und Werkstoff* (50), pp. 191 – 194

Noguchi, M., Fujii, Y., Owada, M., Imamura, Y., Tokoro, M., Tooya, R. (1991): AE monitoring to detect termite attack on wood of commercial dimension and posts. *Forest Products Journal* 41(9): pp. 32 – 36

Patton-Mallory, M., De Groot, R. C. (1989): Acousto-ultrasonics for evaluating decayed wood products. *Proceedings Pacific Timber Eng. Conf.*, Vol. 2, pp. 185 – 190

Pellerin, R. F. (1989): Inspection of wood structures for decay using stress waves. *Proceedings Pacific Timber Eng. Conf.*, Vol. 2, pp. 191 – 195

Porter, A. W. (1964): On the mechanics of fracture in wood. Ph. D. Thesis, State Univ. College For., Syracuse University

Porter, A. W., El-Osta, M. L., Kusec, D. J. (1972): Prediction of failure of finger joints using acoustic emissions. *Forest Products Journal*, Vol. 22, No. 9, pp. 74 – 82

Reinhardt, H. W., Hordijk, D. A. (1988): Various techniques for the assessment of the damage zone between two saw cuts. France – US workshop »Strain localisation and size effect due to cracking and damage.« Cachan, Sept. 6 – 9

RILEM TC 50 – FMC (1985). Determination of the fracture energy of mortar and concrete by means of three-point bending tests of notched beams. *Materials and Structures* 18, pp. 285 – 290

Sato, K., Fushitani, M., Noguchi, M. (1984): Discussion of tensile fracture of wood using acoustic emissions. Estimation of tensile strength and consideration of AE generation based on fracture mechanics. *Mokuzai Gakkaishi, Journal Japan Wood Research Soc.* 30 (2): 117 – 123

- [12] Fehlhaber, T., Reinhardt, H.W., Drawer, O., Sosoro, M. and Krumpe, A.:
Transportphänomene organischer, wasserlöslicher Flüssigkeiten in Beton.
DFG Re 691/4-1 Report, 1991
- [13] Saechtling, H.:
Kunststoff-Taschenbuch.
Hanser Verlag München, 1979